

University of Groningen

## Rapid amplitude-phase reconstruction of femtosecond pulses from intensity autocorrelation and spectrum

Baltuška, Andrius; Pugžlys, Audrius; Pshenichnikov, Maxim S.; Wiersma, Douwe A.

*Published in:*

Summaries of Papers Presented at the Conference on Lasers and Electro-Optics, 1999. CLEO '99

**IMPORTANT NOTE: You are advised to consult the publisher's version (publisher's PDF) if you wish to cite from it. Please check the document version below.**

*Document Version*

Publisher's PDF, also known as Version of record

*Publication date:*

1999

[Link to publication in University of Groningen/UMCG research database](#)

*Citation for published version (APA):*

Baltuška, A., Pugžlys, A., Pshenichnikov, M. S., & Wiersma, D. A. (1999). Rapid amplitude-phase reconstruction of femtosecond pulses from intensity autocorrelation and spectrum. In *Summaries of Papers Presented at the Conference on Lasers and Electro-Optics, 1999. CLEO '99* (pp. 264-265). University of Groningen, The Zernike Institute for Advanced Materials.

### Copyright

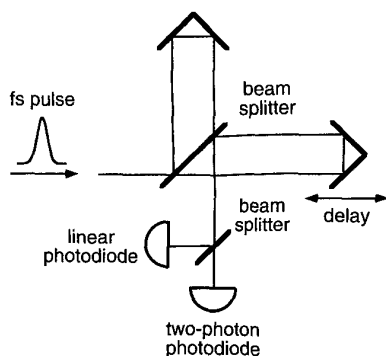
Other than for strictly personal use, it is not permitted to download or to forward/distribute the text or part of it without the consent of the author(s) and/or copyright holder(s), unless the work is under an open content license (like Creative Commons).

The publication may also be distributed here under the terms of Article 25fa of the Dutch Copyright Act, indicated by the "Taverne" license. More information can be found on the University of Groningen website: <https://www.rug.nl/library/open-access/self-archiving-pure/taverne-amendment>.

### Take-down policy

If you believe that this document breaches copyright please contact us providing details, and we will remove access to the work immediately and investigate your claim.

Downloaded from the University of Groningen/UMCG research database (Pure): <http://www.rug.nl/research/portal>. For technical reasons the number of authors shown on this cover page is limited to 10 maximum.



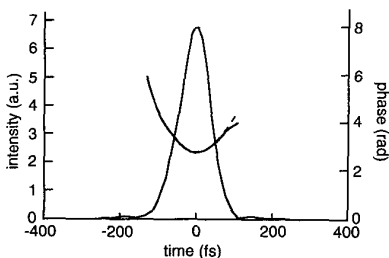
CWF21 Fig. 1. Experimental set-up.

relation signal generated by nonlinear wave mixing. As discussed in Ref. 2, nonlinear wave mixing has the following disadvantages: (1) To measure sub-50-fs pulses, a crystal as thin as several tens of micrometers is required to avoid dispersion-induced pulse broadening and to ensure a sufficiently broad phase-matching bandwidth. (2) Wave mixing in thin nonlinear crystals is intrinsically an inefficient process. This sets a limit on the sensitivity. We developed a phase-retrieval waveform measurement technique by using only photodiodes. Because the nonlinear signal was obtained from two-photon-induced photocurrent,<sup>2</sup> the above disadvantages were eliminated.

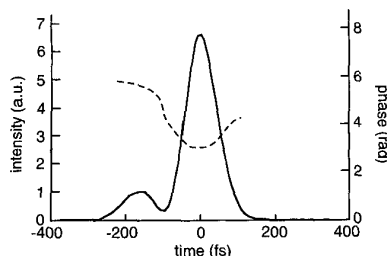
The experimental set-up is shown in Fig. 1. When the optical delay line is scanned, the output of the linear silicon photodiode oscillates at a period of  $\lambda/2$ . The oscillating signal is the field autocorrelation  $G_1(\tau)$ . In the mean time the output from the GaAsP two-photon photodiode oscillates at a period of  $\lambda/4$ . The oscillating signal is the second-harmonic field autocorrelation  $F_{SH}(\tau)$ :

$$F_{SH}(\tau) = \int E^2(t)E^{*2}(t - \tau)dt. \quad (1)$$

The  $\lambda/4$  oscillating signal sits on a slowly varying background, which is the intensity autocorrelation  $G_2(\tau)$ . After Fourier transformation,  $G_1(\tau)$  gives  $|E(\omega)|$ , the power spectrum of  $E(t)$ ;  $G_2(\tau)$  gives  $|I(\omega)|$ , the power spectrum of  $I(t)$ ; and  $F_{SH}(\tau)$  gives  $|U(\omega)|$ , the power spectrum of  $E^2(t)$ . It has been shown that  $|E(\omega)|$ ,  $|I(\omega)|$ , and  $|U(\omega)|$  together contain enough in-



CWF21 Fig. 2. Solid lines: The retrieved intensity and phase profiles of pulses after passing through 2.5-cm BK7 glass. Dashed line: the expected phase profile.



CWF21 Fig. 3. Solid line: The retrieved intensity profile of a double-peak pulse. Dashed line: the retrieved phase profile.

formation to determine the field distribution  $E(t)$ , up to the time-reversal ambiguity.<sup>3</sup> Our phase-retrieval algorithm starts from the measured  $|E(\omega)|$  and an initial guess of the phase  $\phi(\omega)$ , which generate the trial field  $E_i(t)$ . From  $E_i(t)$  we calculate  $I_i(\omega)$  and  $U_i(\omega)$ . By retaining their phases while replacing the calculated  $|I_i(\omega)|$  and  $|U_i(\omega)|$  with measured data, we approach the actual  $E(t)$  by iteration. Near the end of iteration, when the improvement slows down, we speed up the convergence by using the functional derivative with respect to  $\phi(\omega)$  to minimize the difference between the calculated and the measured  $G_2(\tau)$  and  $F_{SH}(\tau)$ .

We use pulses synthesized from a transform-limited Kerr-lens mode-locked Ti:sapphire laser to verify the effectiveness of this method. Figure 2 shows the intensity and phase of the pulses after propagating through 2.5-cm BK7 glass. The measured phase curvature and the change of pulse duration agree well with the expected waveform calculated from dispersion data. To show the capability of the method in measuring complex waveforms, we use a double-peak waveform, which is known to be a difficult case for FROG,<sup>4</sup> for the test. The double-peak pulses are synthesized by splitting the pulses at a 1:7 power ratio, delaying the smaller one by 150 fs, passing the larger one through 2.5-cm BK7 glass, then recombining them before the measurement. Figure 3 shows the retrieved double-peak waveform. The errors of the retrieved power ratio and delay are less than 4%.

The sensitivity of this method is great enough for measuring the waveform of nanojoule pulses stretched to hundreds of picoseconds. This makes it a convenient tool for characterizing amplifier seeds and synthesized pulses. The set-up is also simple enough that the whole system can be fabricated as a standard part of femtosecond lasers.

\*Department of Physics, National Taiwan University

\*\*Institute of Atomic and Molecular Sciences, Academia Sinica, Taipei, Taiwan

†Also with the Institute of Atomic and Molecular Sciences, Academia Sinica

1. D.J. Kane and R. Trebino, *Opt. Lett.* **18**, 823 (1993).
2. J.K. Ranka, *et al.*, *Opt. Lett.* **22**, 1344 (1997).
3. K. Naganuma, *et al.*, *IEEE J. Quantum Electron.* **25**, 1225 (1989).
4. K.W. DeLong and R. Trebino, *J. Opt. Soc. Am. A* **11**, 2429 (1994).

## CWF22

## Rapid amplitude-phase reconstruction of femtosecond pulses from intensity autocorrelation and spectrum

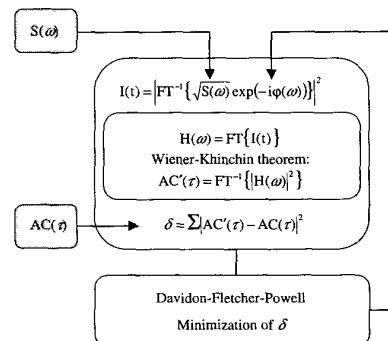
Andrius Baltuska, Audrius Pugžlys, Maxim S. Pshenichnikov, Douwe A. Wiersma, *Ultrafast Laser and Spectroscopy Laboratory, Department of Chemistry, University of Groningen, Nijenborgh 4, 9747 AG Groningen, The Netherlands; E-mail: A.Baltuska@chem.rug.nl*

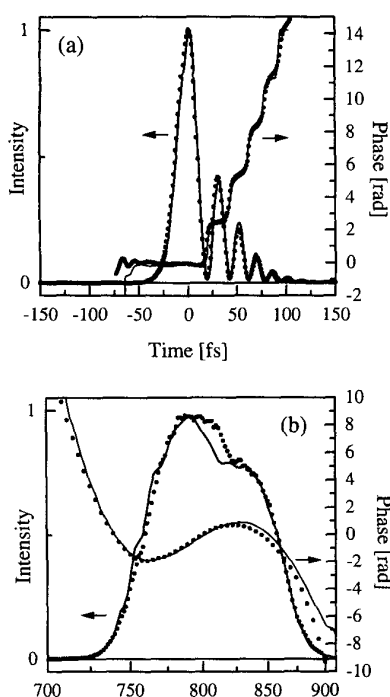
The retrieval of time-dependent intensity and phase of femtosecond laser pulses is a long-standing problem. To the date, frequency-resolved optical gating (FROG)<sup>1</sup> is probably the most trustworthy pulse measurement method. However, it requires a substantial experimental and numerical involvement. This motivates the quest for other simpler high-fidelity pulse measuring techniques.

In this contribution we present a new method of deciphering the pulse structure from the intensity autocorrelation trace  $AC(\tau)$  and the intensity spectrum  $S(\omega)$ . We show that such a set of data is sufficient to restore the intensity and phase of a femtosecond pulse except for the typical uncertainties concerning the time shift and direction. The main feature of the proposed method is its robustness and swift convergence. Unlike a two-step pulse reconstruction,<sup>2</sup> our algorithm employs the time- and frequency-domain data simultaneously, which in general<sup>3</sup> provides a much faster convergence.

The input data are converted into two arrays each containing  $N$  data points (Fig. 1). The iterative algorithm attempts to obtain the best match for the measured autocorrelation trace by varying the spectral phase  $\phi(\omega)$ . The rms difference  $\delta$  (the algorithm error) between the input autocorrelation trace and the one computed for the current guess of  $\phi(\omega)$  is minimized by Davidon-Fletcher-Powell variable metric method.<sup>4</sup> A successful convergence of the iterative algorithm results in the complete amplitude and phase reconstruction of the pulse. The proposed method is incredibly fast because it employs one-dimensional Fourier transforms.

To prevent possible algorithm stagnation, we represent  $\phi(\omega)$  by a cubic spline drawn through  $m$  ( $m < N$ ) selected values of the

CWF22 Fig. 1. Schematic of the iterative algorithm for pulse characterization from intensity autocorrelation  $AC(\tau)$  and spectrum  $S(\omega)$ .



CWF22 Fig. 2. Comparison of intensity and phase retrieved by SHG FROG (solid curves) and the proposed algorithm (solid circles) in the time (a) and frequency (b) domains.

spectral phase (nodes). Resampling of the nodes provides a boost necessary to avoid algorithm stagnation. Consequently, the algorithm can be initiated with a modest amount of nodes since it self-adjusts to the complexity of the pulse by automatic run-time incrementing of  $m$ . The influence of each node on  $\varphi(\omega)$  is localized to the two adjacent spline segments on each side of the node. Thus, the required for minimization independence of  $m$  parameters and the continuity of  $\varphi(\omega)$  are both achieved at the same time.

We applied the developed method to characterize in real time the output of a 10-fs Ti:sapphire oscillator. The different pulse shapes were tailored by manipulating dispersion outside the cavity. The autocorrelations were measured by using two-photon-induced current in a GaAsP photodiode<sup>5</sup> to provide adequately broadband second-order response. All reconstructed pulses correspond very well to the results of independent SHG FROG characterization. As an example, Fig. 2 shows the case of a strong satellite structure on the pulse, which has been shown to confuse the earlier algorithm.<sup>2</sup>

We also address the experimental and numerical issues, such as spectral filtering in the autocorrelator, the required dynamic range and signal-to-noise ratio, convergence stability and the choice of initial guess.

1. D.J. Kane and R. Trebino, IEEE J. Quantum Electron. **29**, 571 (1993).
2. J. Peatross and A. Rundquist, J. Opt. Soc. Am. B. **15**, 216 (1997).
3. J.R. Fienup, Appl. Opt. **21**, 2758 (1982).
4. W.H. Press, S.A. Teukolsky, W.T. Vetter-

ling, and B.P. Flannery, Numerical Recipes in C: The Art Of Scientific Computing, 2<sup>nd</sup> ed. (Cambridge University, 1992) P. 425.

5. J.K. Ranka *et al.*, Opt. Lett. **22**, 1344 (1997).

## Materials for Nonlinear Optical Applications

### CWF23

#### Conformational dependence and femtosecond response of the third-order nonlinearity in retinal derivatives

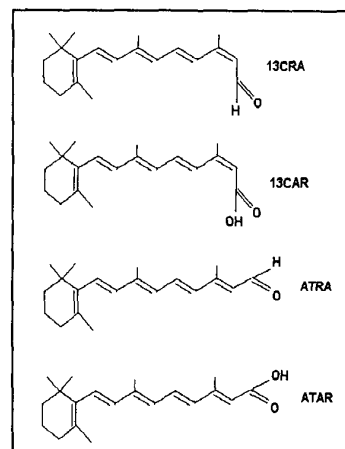
A.G. Bezerra, Jr, A.S.L. Gomes, D.A. da Silva-Filho, Cid B. de Araújo, C.P. de Melo, Departamento de Física, Universidade Federal de Pernambuco, 50670-901, Recife, PE, Brasil; E-mail: arandi@df.ufpe.br

The nonlinear optical properties of organic materials have been thoroughly studied with views to the basic understanding of its physical origin as well as to their application in photonic devices. It is the  $\pi$ -electron delocalization in organic molecules that leads to high molecular hyperpolarizabilities and large nonlinear susceptibilities.

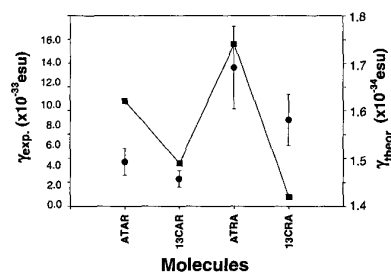
Retinal—a molecular structure related to vitamin A—and its derivatives belong to a family of molecules that plays a prevalent role in photobiological processes.<sup>1</sup> For instance, the primary event of vision mechanism in animals is associated to the *cis* to *trans* isomerization of the retinal molecule. Toto and coworkers<sup>2</sup> have predicted that this conformational change should be accompanied by a noticeable change in the hyperpolarizability of the molecules since the more linear character of the *trans* conformation should favor the delocalization of the  $\pi$ -electrons in the conjugated system.

We used the Z-scan technique<sup>3</sup> to determine the nonlinear refractive index,  $n_2$ , and the nonlinear absorption coefficient,  $\alpha_2$ , of 13-*cis* retinal aldehyde (13CRA), 13-*cis* retinoic acid (13CAR), *all-trans* retinal aldehyde (ATRA) and *all-trans* retinoic acid (ATAR), and then infer the change in the nonlinearity due to a conformational dependence. The second harmonic of a cw pumped Q-switched and mode-locked Nd:YAG laser delivering pulses of 70 ps (FWHM) at 532 nm was used. A single pulse at 10 Hz was selected using a "pulse picker." From the measured values of  $n_2$  and  $\alpha_2$  we have determined the values of  $\chi^{(3)}$  and, therefore, of the second hyperpolarizability,  $\gamma$ . This is achieved through  $\chi^{(3)} = Nf^4\gamma$ , where  $f$  is a local field correction factor and  $N$  is the number of molecules per unit volume.

The molecular structures of the retinal derivatives are shown in Fig. 1(a). To get a better understanding of the microscopic origin of the nonlinearity, we have compared our experimentally measured values of  $\gamma$  with those resulting from an AM1-TDHF quantum-chemical calculation for the molecules studied in this work, and found a general agreement between the experimental and theoretical trends as shown in Fig. 1(b). For both retinal aldehyde and retinoic acid the hyperpolariz-



(a)

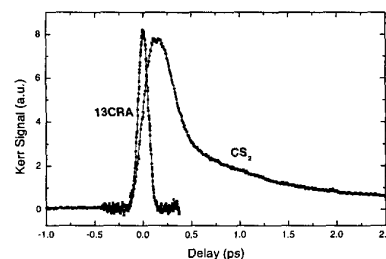


(b)

CWF23 Fig. 1. (a) Molecular structure of the retinal derivatives: 13-*cis* retinal aldehyde (13CRA), 13-*cis* retinoic acid (13CAR), *all-trans* retinal aldehyde (ATRA) and *all-trans* retinoic acid (ATAR). (b) Plot of experimentally determined,  $\gamma_{exp}$ , (circles), and theoretically AM1-TDHF calculated,  $\gamma_{theor}$ , (squares), values of the retinal derivatives studied.

abilities of the *trans* molecules are greater than those of the corresponding *cis* isomer, a result that can be understood considering the more linear character of the *trans* conformation, as theoretically predicted.<sup>2</sup>

Temporal measurements using the Optical Kerr Gate method were performed with 60 fs pulses from a Ti:Sapphire laser operating at 800 nm. The results indicate that the response time of the material is shorter than 60 fs (Fig.



CWF23 Fig. 2. Optical Kerr Gate signal of retinal derivative 13CRA (dissolved in chloroform) and CS<sub>2</sub>. Note the faster response time of the 13CRA molecules in comparison with the CS<sub>2</sub> response.